JACS
JOURNAL OF THE AMERICAN CHEMICAL SOCIETY
Communication
pubs.acs.org/JACS

Two-Dimensional Semiconducting Boron Monolayers

Shao-Gang Xu,[†,‡,#] Xiao-Tian Li,[†,#] Yu-Jun Zhao,[†] Ji-Hai Liao,[†] Wang-Ping Xu,[‡] Xiao-Bao Yang,*[,†] and Hu Xu*[,‡]

[†]Department of Physics, South China University of Technology, Guangzhou 510640, People's Republic of China
[‡]Department of Physics, South University of Science and Technology of China, Shenzhen 518055, People's Republic of China

Supporting Information

ABSTRACT: The two-dimensional boron monolayers were reported to be metallic both in previous theoretical predictions and experimental observations. Unexpectedly, we have first found a family of boron monolayers with the novel semiconducting property as confirmed by the first-principles calculations with the quasi-particle G_0W_0 approach. We demonstrate that the connected network of hexagonal vacancies dominates the gap opening for both the in-plane $s+p_{x,y}$ and p_z orbitals, with which various semiconducting boron monolayers are designed to realize the band gap engineering for the potential applications in electronic devices. The semiconducting boron monolayers in our predictions are expected to be synthesized on the proper substrates, due to the similar stabilities to the ones observed experimentally.

Graphene,[1] a free-standing two-dimensional (2D) carbon (C) exfoliated from the bulk phase, has provoked a rush of attention. However, the intrinsic metallicity of graphene prevents its application to practical nanodevices, and various means have been proposed to introduce a suitable band gap for graphene, such as the chemical functionalization (hydrogenated graphene)[2] and physical cutting (graphene nanoribbons).[3] Recently, the few-layer black phosphorus is attractive due to their semiconducting characteristic,[4] where the atomic structures can be theoretically determined through the relaxation from the layered bulk counterpart.[5]

Boron (B), one of C's nearest neighbors in the periodic table, demonstrates the polymorphism in low-dimensional structures[6−8] due to the multicenter bonds, leading to the diverse properties. Experimental observations show that small B_n clusters are planar triangular fragments;[9] however, the corresponding boron monolayers have been found to be not stable due to the large deformation and buckling.[10] Inspired by the computational prediction of B_{80},[11] the stable boron monolayers with hexagonal vacancies have been proposed,[12,13] leading to extensive searches focusing on the concentration and distribution of vacancies.[14,15] Further experimental observation of B_{36} confirms that hexagonal vacancies are important in stabilizing the larger planar B clusters to be considered as the precursor for boron monolayers.[16] In addition, the B_{35}^- with a double-hexagonal vacancy may be another flexible motif to build various boron monolayers,[17,18] which are supposed to be synthesized on the proper metal surfaces.[19] Recently, two research groups have independently reported that the boron monolayers could be fabricated on the silver (Ag) substrates by the molecular beam epitaxy (MBE) method.[20,21] Theoretically, the detailed atomic structures of boron monolayers are confirmed by the first-principles calculations,[22,23] where a penetration mechanism of initial nucleation is especially proposed.[22]

As is known, the polymorphism of boron monolayers will induce the variety of properties, including the unusual Dirac Fermions,[24] and the coexisting Dirac nodal lines and tilted semi-Dirac cones.[25] During the growth of boron monolayers, the metallic B nanoribbons (BNRs) have been found across the steps on the Ag substrates.[26] To our knowledge, there are only few B periodical structures predicted to be semiconducting. In addition to the one-dimensional (1D) B nanotubes with small diameters,[13] only one intrinsic BNR with armchair edges[27] has been predicted to be semiconducting, and the 1D B chains[28] will undergo a metal−semiconductor transition due to the mechanism of spin density wave. Until now, the planar boron monolayers are concluded to be metallic[7,14,29] by experiments and theories, characterized by the out-of-plane p_z-derived bands. However, it is not clear whether there are any semiconducting boron monolayers, the confirmation of which will extend our understanding of 2D boron.

In this work, we have theoretically shown that the in-plane $s+p_{x,y}$ orbitals and p_z-derived bands in boron monolayers could be effectively modulated by the connected network of hexagonal vacancies, which results in a family of semiconducting boron monolayers as confirmed by the first-principles calculations. We have found a simple rule to construct semiconducting boron monolayers for the realization of band gap engineering, indicating a brand new platform for the potential applications in electronic devices.

The first-principles calculations were performed based on density-functional theory (DFT) with the projected augmented wave (PAW)[30] scheme, as implemented in Vienna *ab initio* simulation package (VASP)[31] (details in the Supporting Information). The Heyd−Scuseria−Ernzerhof (HSE06) hybrid functional[32] and the quasi-particle G_0W_0 approach[33] were applied for the band gap corrections. Thermal stability was studied using *ab initio* molecular dynamics (AIMD) simulations with the temperature controlled by a Nosé heat bath scheme.[34] The climbing image nudged elastic band method (CI-NEB)[35] was adopted to study the migration pathways of B atoms in boron monolayers.

Received: August 15, 2017
Published: November 16, 2017

DOI: 10.1021/jacs.7b08680
J. Am. Chem. Soc. 2017, 139, 17233−17236

As shown in Figure 1a, the first semiconducting boron monolayer (β_1^s) possesses the connected network of hexagonal

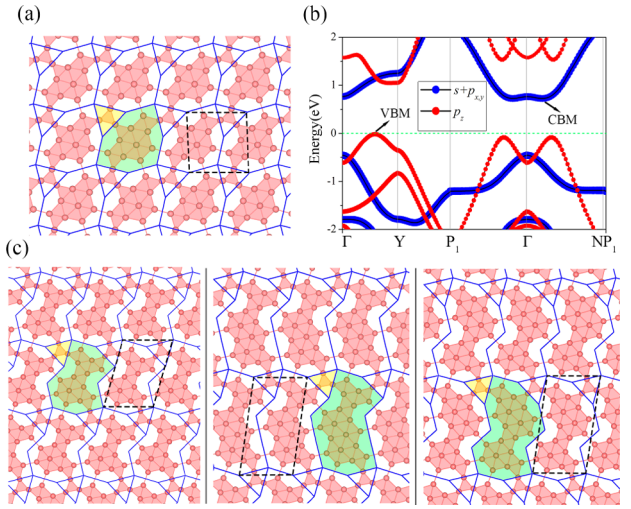

Figure 1. Atomic structures and band structure for the semiconducting boron monolayers. Panels a and b represent the atomic structure and HSE06 band structure of the β_1^s boron monolayer. (VBM is set to 0.) Panel c represents the atomic structures of the three semiconducting boron monolayers (β_{a1}^s, β_{a2}^s, β_{a3}^s). The blue solid lines represent the connecting lines of the hexagonal vacancies. The black dash lines represent the unit cells of the corresponding boron monolayers.

vacancies which can be divided into the triangle regions (TriRs) and the heptagon regions (HepRs), where the real space structural parameters after relaxation are listed in Table S1. The HSE06 band structure calculation (see Figure 1b) confirms that this boron monolayer is semiconducting with an indirect gap of 0.741 eV. The projected band structure reveals that the valence band maximum (VBM) is dominated by the out-of-plane p_z orbitals while the conduction band minimum (CBM) is attributed to the in-plane $s+p_{x,y}$ orbitals. According to the calculated phonon dispersion (see Figure S1b), no imaginary phonon modes are found in the whole first Brillouin zone, indicating the kinetic stability of the new boron monolayer. We also assessed the thermal stability of the boron monolayer by performing AIMD simulation at the temperature of 500 K with the time step of 1 fs. The structural snapshot of the supercell at 10 ps (shown in Figure S1c) reveals that the semiconducting boron monolayer has a good thermodynamic stability, which can maintain the structural integrity in room-temperature environment. In addition, we have found three semiconducting boron monolayers assembled by the triangle regions and irregular polygon regions shown in Figure 1c, and the corresponding band structures are shown in Figure S2.

In the heptagon region of β_1^s, there is a unit cell of β sheet.[12] Thus, we can construct a family potential semiconducting boron monolayers by increasing the number of β unit cell (β-UC) included in the HepRs (shown in Figure 2a). The named β_m^s boron monolayer is one with m β-UC in the heptagon regions, where there is one β-UC in the HepRs of the β_1^s boron monolayer (shown in Figure 1a) with the least number of atoms. Under the mentioned definition, we can obtain the β_2^s boron monolayer with two β-UC assembled in the HepRs, as well as the β_3^s boron monolayer in the similar way. Furthermore, the $\beta_{2,3}^s$ boron monolayer is the hybrid structure of β_2^s and β_3^s. The structural parameters of these three new

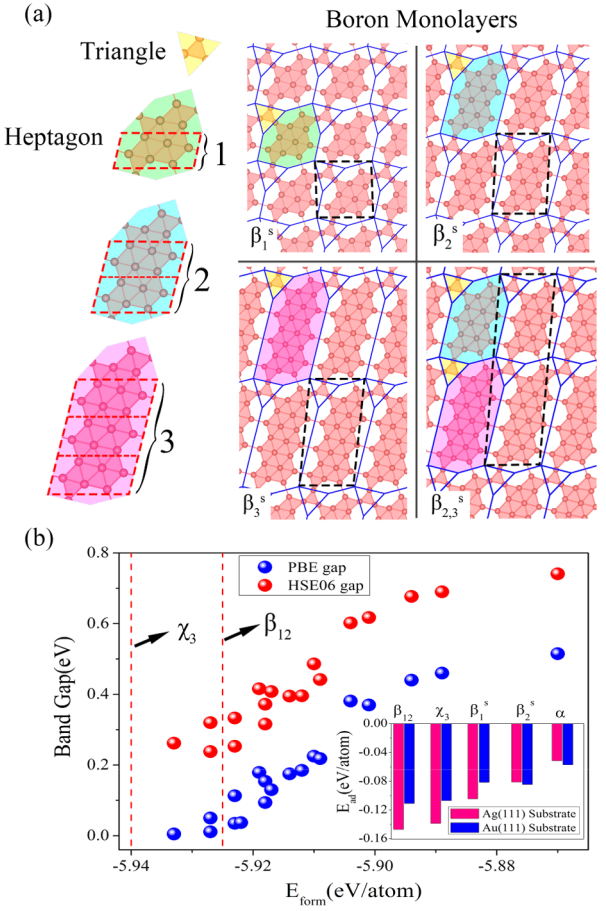

Figure 2. Combination rule and atomic structures of the semiconducting boron monolayers. (a) Schematic diagram of the combination rule for the semiconducting boron monolayers (β_m^s (m = 1−3) and $\beta_{2,3}^s$). The blue solid lines represent the connecting lines of the hexagonal vacancies. The black dash lines represent the unit cells of the corresponding boron monolayers. The red dash lines represent the unit cell of β sheet. (b) Relationship of band gaps and average formation energy (E_{form}) for the new designed semiconducting boron monolayers. The inset represents the average adsorption energy (E_{ad}) of boron monolayers on the Ag/Au(111) substrates.

boron monolayers with the same space group of $Pm(6)$ are presented in Table S1. There are no imaginary phonon modes along all the high-symmetry lines (see Figure S3), and the calculated diffusion barriers of the B atoms in the TriRs are larger than 1 eV (shown in Figure S4). Furthermore, the AIMD simulations in Figure S5 show that the semiconducting boron monolayers can maintain their frameworks at 700 K, which indicate that the boron monolayers should have high dynamic and thermal stabilities.

The HSE06 band structures (shown in Figure S6) show that the above boron monolayers are semiconducting with the band gaps of 0.602, 0.416, and 0.396 eV, respectively. The β_2^s boron monolayer is an indirect gap semiconductor with the VBM is along M-Γ, and the CBM is located at Γ point. Notably, the β_3^s boron monolayer is a semiconductor with a direct gap, where both the VBM and CBM are located at Y point. The $\beta_{2,3}^s$ boron monolayer is an indirect gap semiconductor with the VBM is along Γ-X, and the CBM is located at Y point. Checking the projected orbitals plotted in the band structures, we can see that the VBM and CBM are contributed by the in-plane $s+p_{x,y}$ orbitals for the β_2^s, β_3^s, and $\beta_{2,3}^s$ boron monolayers. Similar to the

DOI: 10.1021/jacs.7b08680
J. Am. Chem. Soc. 2017, 139, 17233−17236

α sheet,[12] there are gaps for in-plane $s+p_{x,y}$ orbitals near the Fermi level (E_F) in a few previously proposed stable boron monolayers, whereas the p_z orbitals account for their metallicity. Interestingly, our proposed boron monolayers open the energy gaps of $s+p_{x,y}$ and p_z orbitals near the E_F level.

As the number of β-UC in the HepRs increases, the band structures and the PDOS analysis (shown in Figure S7) indicate that the systems become metallic gradually, where the bands near the E_F level are attributed to the in-plane $s+p_{x,y}$ orbitals rather than the p_z orbitals. The connected network of hexagonal vacancies is dominant to the gap opening for both $s+p_{x,y}$ and p_z orbitals in the semiconducting boron monolayers. Because the charge distributions of the valence bands (shown in Figure S8) are moving from the TriRs chains to the β BNRs regions with the increasing of the number of β-UC, which leads to the closing of the energy gaps for $s+p_{x,y}$ and p_z orbitals in β^s_m boron monolayers with $m \geq 6$. By the combinations ($\beta^s_{m1,m2,m3,...}$ (mi = 1−5)) in the HepRs, we have constructed a family of semiconducting boron monolayers with various band gaps (shown in Table S2), indicating the realization of the band gap engineering. As shown in Figure 2b, at a fixed vacancy concentration we can construct different structures with various band gaps, and the average formation energy (E_{form}) of a few semiconducting boron monolayers are in the region between the experimentally[21] synthesized β_{12} (−5.925 eV/atom) and χ_3 (−5.940 eV/atom) sheets. There is a variation of boron monolayers' stabilities as a function of the metal substrates (shown in Figures S9−S11). In addition, the differences of the average adsorption energy between semiconducting (β^s_1, β^s_2) and (β_{12}, χ_3) on the Ag(111) substrate are about 40 meV/atom, which will be reduced to be within 30 meV/atom for Au(111) substrate (shown in the inset of Figure 2b). Note that the semiconducting boron monolayers are more stable than the experimental metastable α sheet[36] on both Ag(111) and Au(111) substrates, indicating the possible synthesis by the control of growth conditions. On the Cu(111) substrate, β^s_1 is of similar stability to χ_3 and it will become more stable than β_{12} on the Ni(111) substrate (as shown Figure S11), though the larger adsorption energy might induce difficulty in the exploitation from the substrates. It is expected that the Au−Cu alloys might be a suitable substrate to synthesize the semiconducting boron monolayers to avoid the larger adhesion energy of boron monolayers on substrates.

The direct band gap characteristic of β^s_3 boron monolayer can be potentially applied in the infrared optoelectronic devices and field-effect transistor. The G_0W_0 calculation (shown in Figure 3a) predicts that the fundamental band gap of β^s_3 boron monolayer is 0.484 eV, which maintains the characteristic of direct gap at Y point with a linear increasing as the biaxial strain ($-3\% \leq \sigma \leq +3\%$). The semiconducting characteristic in boron monolayers is expected to be robust against the strain induced by the substrate and the band gaps could be effectively modulated by means of the biaxial strain. As shown in Figure 3b, the band decomposed charge distributions of VBM and CBM for β^s_3 are found to be mainly contributed to the in-plane sp^2 hybrid orbitals, which are located in TriRs. Therefore, we confirm that the vanished metallicity characterized by the gap opening in both in-plane sp^2 and p_z orbitals is attributed to the connected network of hexagonal vacancies with the motif of TriRs.

In summary, we have demonstrated a family of boron monolayers with the novel semiconducting property for the first time, attributed to both the in-plane $s+p_{x,y}$ and the p_z-derived bands modulated by the connected network of hexagonal vacancies. The proposed semiconducting boron monolayers may be synthesized on the proper substrates, because they are of similar stability to those observed experimentally. For the boron monolayer with a direct gap, mechanical biaxial strains within a small region may induce a linear tuning of the band gap, indicating a brand new platform for the potential applications in electronic devices.

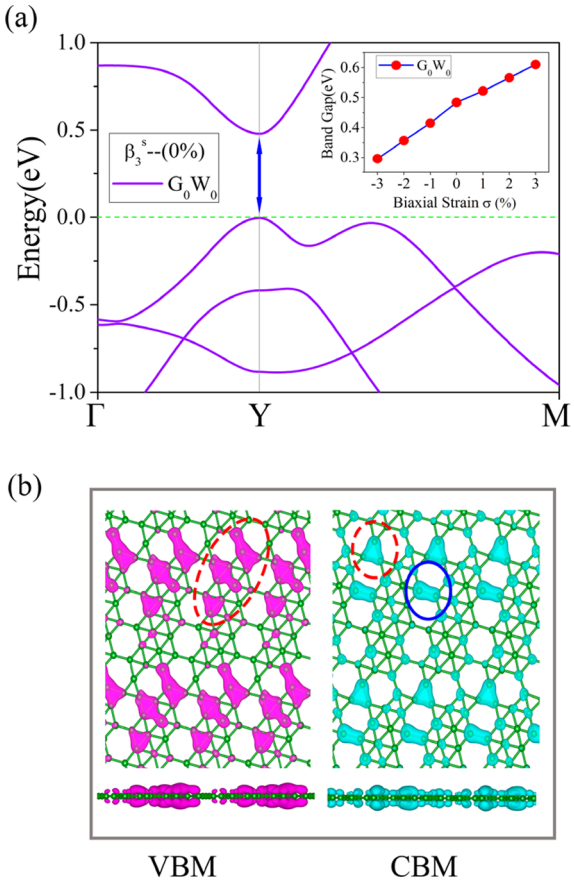

Figure 3. Electronic properties of β^s_3 boron monolayer. (a) G_0W_0 band structure of β^s_3 boron monolayer (VBM is set to 0), and the inset represents the relation of G_0W_0 band gaps and biaxial strain. (b) Band decomposed charge densities of β^s_3 boron monolayer at VBM and CBM.

■ ASSOCIATED CONTENT

Supporting Information

The Supporting Information is available free of charge on the ACS Publications website at DOI: 10.1021/jacs.7b08680.

AIMD simulation results; phonon dispersion spectras; NEB diffusion path; band structures; PDOS analysis; band decomposed charge densities; adsorption on the metal substrates; tables of stabilities and band gaps (PDF)

■ AUTHOR INFORMATION

Corresponding Authors

*scxbyang@scut.edu.cn

*xuh@sustc.edu.cn

ORCID

Xiao-Bao Yang: 0000-0001-8851-1988

Hu Xu: 0000-0002-2254-5840

DOI: 10.1021/jacs.7b08680
J. Am. Chem. Soc. 2017, 139, 17233−17236

Author Contributions

[#]S.-G.X. and X.-T.L. contributed equally to this work.

Notes

The authors declare no competing financial interest.

■ ACKNOWLEDGMENTS

This work was supported by the National Natural Science Foundation of China (Nos. 11474100, 11674148, 11574088), Guangdong Natural Science Funds for Distinguished Young Scholars (Nos. 2014A030306024, 2017B030306008), the Basic Research Program of Science, Technology and Innovation Commission of Shenzhen Municipality (Grant No. JCYJ20160531190054083), and the Foundation for Innovative Research Groups of the National Natural Science Foundation of China (Grant No. 51621001).

■ REFERENCES

(1) Castro Neto, A. H.; Guinea, F.; Peres, N. M. R.; Novoselov, K. S.; Geim, A. K. *Rev. Mod. Phys.* **2009**, *81*, 109.
(2) Fiori, G.; Lebègue, S.; Betti, A.; Michetti, P.; Klintenberg, M.; Eriksson, O.; Iannaccone, G. *Phys. Rev. B: Condens. Matter Mater. Phys.* **2010**, *82*, 153404.
(3) Son, Y.-W.; Cohen, M. L.; Louie, S. G. *Phys. Rev. Lett.* **2006**, *97*, 216803.
(4) Li, L. K.; Yu, Y. J.; Ye, G. J.; Ge, Q. Q.; Ou, X. D.; Wu, H.; Feng, D. L.; Chen, X. H.; Zhang, Y. B. *Nat. Nanotechnol.* **2014**, *9*, 372.
(5) Bhimanapati, G. R.; Lin, Z.; Meunier, V.; Jung, Y.; Cha, J.; Das, S.; Xiao, D.; Son, Y.; Strano, M. S.; Cooper, V. R.; Liang, L.; Louie, S. G.; Ringe, E.; Zhou, W.; Kim, S. S.; Naik, R. R.; Sumpter, B. G.; Terrones, H.; Xia, F.; Wang, Y.; Zhu, J.; Akinwande, D.; Alem, N.; Schuller, J. A.; Schaak, R. E.; Terrones, M.; Robinson, J. A. *ACS Nano* **2015**, *9*, 11509.
(6) Wang, L. S. *Int. Rev. Phys. Chem.* **2016**, *35*, 69.
(7) Zhang, Z.; Penev, E. S.; Yakobson, B. I. *Nat. Chem.* **2016**, *8*, 525.
(8) Xu, S.-G.; Zhao, Y.-J.; Liao, J.-H.; Yang, X.-B. *J. Chem. Phys.* **2015**, *142*, 214307.
(9) Zhai, H. J.; Kiran, B.; Li, J.; Wang, L. S. *Nat. Mater.* **2003**, *2*, 827.
(10) Kunstmann, J.; Quandt, A. *Phys. Rev. B: Condens. Matter Mater. Phys.* **2006**, *74*, 035413.
(11) Gonzalez Szwacki, N.; Sadrzadeh, A.; Yakobson, B. I. *Phys. Rev. Lett.* **2007**, *98*, 166804.
(12) Tang, H.; Ismail-Beigi, S. *Phys. Rev. Lett.* **2007**, *99*, 115501.
(13) Yang, X.; Ding, Y.; Ni, J. *Phys. Rev. B: Condens. Matter Mater. Phys.* **2008**, *77*, 041402.
(14) Penev, E. S.; Bhowmick, S.; Sadrzadeh, A.; Yakobson, B. I. *Nano Lett.* **2012**, *12*, 2441.
(15) Wu, X.; Dai, J.; Zhao, Y.; Zhuo, Z.; Yang, J.; Zeng, X. C. *ACS Nano* **2012**, *6*, 7443.
(16) Piazza, Z. A.; Hu, H. S.; Li, W. L.; Zhao, Y. F.; Li, J.; Wang, L. S. *Nat. Commun.* **2014**, *5*, 3113.
(17) Li, W. L.; Chen, Q.; Tian, W. J.; Bai, H.; Zhao, Y. F.; Hu, H. S.; Li, J.; Zhai, H. J.; Li, S. D.; Wang, L. S. *J. Am. Chem. Soc.* **2014**, *136*, 12257.
(18) Sergeeva, A. P.; Popov, I. A.; Piazza, Z. A.; Li, W. L.; Romanescu, C.; Wang, L. S.; Boldyrev, A. I. *Acc. Chem. Res.* **2014**, *47*, 1349.
(19) Zhang, Z.; Yang, Y.; Gao, G.; Yakobson, B. I. *Angew. Chem., Int. Ed.* **2015**, *54*, 13022.
(20) Mannix, A. J.; Zhou, X.-F.; Kiraly, B.; Wood, J. D.; Alducin, D.; Myers, B. D.; Liu, X.; Fisher, B. L.; Santiago, U.; Guest, J. R.; Yacaman, M. J.; Ponce, A.; Oganov, A. R.; Hersam, M. C.; Guisinger, N. P. *Science* **2015**, *350*, 1513.
(21) Feng, B. J.; Zhang, J.; Zhong, Q.; Li, W. B.; Li, S.; Li, H.; Cheng, P.; Meng, S.; Chen, L.; Wu, K. H. *Nat. Chem.* **2016**, *8*, 563.
(22) Xu, S. G.; Zhao, Y. J.; Liao, J. H.; Yang, X. B.; Xu, H. *Nano Res.* **2016**, *9*, 2616.
(23) Shu, H.; Li, F.; Liang, P.; Chen, X. *Nanoscale* **2016**, *8*, 16284.
(24) Feng, B.; Sugino, O.; Liu, R.-Y.; Zhang, J.; Yukawa, R.; Kawamura, M.; Iimori, T.; Kim, H.; Hasegawa, Y.; Li, H.; Chen, L.; Wu, K.; Kumigashira, H.; Komori, F.; Chiang, T.-C.; Meng, S.; Matsuda, I. *Phys. Rev. Lett.* **2017**, *118*, 096401.
(25) Zhang, H.; Xie, Y.; Zhang, Z.; Zhong, C.; Li, Y.; Chen, Z.; Chen, Y. *J. Phys. Chem. Lett.* **2017**, *8*, 1707.
(26) Zhong, Q.; Kong, L.; Gou, J.; Li, W.; Sheng, S.; Yang, S.; Cheng, P.; Li, H.; Wu, K.; Chen, L. *Phys. Rev. Materials* **2017**, *1*, 021001.
(27) Saxena, S.; Tyson, T. A. *Phys. Rev. Lett.* **2010**, *104*, 245502.
(28) Liu, M.; Artyukhov, V. I.; Yakobson, B. I. *J. Am. Chem. Soc.* **2017**, *139*, 2111.
(29) Penev, E. S.; Kutana, A.; Yakobson, B. I. *Nano Lett.* **2016**, *16*, 2522.
(30) Kresse, G.; Joubert, D. *Phys. Rev. B: Condens. Matter Mater. Phys.* **1999**, *59*, 1758.
(31) Kresse, G.; Furthmüller, J. *Phys. Rev. B: Condens. Matter Mater. Phys.* **1996**, *54*, 11169.
(32) Heyd, J.; Scuseria, G. E.; Ernzerhof, M. *J. Chem. Phys.* **2003**, *118*, 8207.
(33) Shishkin, M.; Kresse, G. *Phys. Rev. B: Condens. Matter Mater. Phys.* **2006**, *74*, 035101.
(34) Nosé, S. *J. Chem. Phys.* **1984**, *81*, 511.
(35) Henkelman, G.; Uberuaga, B. P.; Jónsson, H. *J. Chem. Phys.* **2000**, *113*, 9901.
(36) Zhong, Q.; Zhang, J.; Cheng, P.; Feng, B.; Li, W.; Sheng, S.; Li, W.; Meng, S.; Chen, L.; Wu, K. *J. Phys.: Condens. Matter* **2017**, *29*, 095002.

DOI: 10.1021/jacs.7b08680
J. Am. Chem. Soc. 2017, 139, 17233−17236